Adsorption of Et_3N and Bu_3N from Toluene onto AgI in the Very Dilute Region: Surface Models and Cross-Sectional Areas

M. Soledade C. S. Santos and Ester F. G. Barbosa*

Departamento de Química e Bioquímica, FCUL, Campo Grande, Edifício C1, Piso 5, 1700 Lisboa, Portugal

Received: January 27, 1998; In Final Form: April 16, 1998

Adsorption isotherms for triethylamine and tributylamine solutions in toluene onto AgI in the very dilute region are presented and treated according to Everett, and Sircar and Myers models. An analysis of molecular orientation in the adsorbed phase and its consequences on the calculated cross-sectional areas for adsorbed molecules is performed, and a simple procedure to calculate cross-sectional areas along different molecular projections, based on basic geometrical shapes, is put forth. The proposed procedure is tested for the adsorption of alkanoic acids on silica and leads to results identical with Meyer's. For spherical molecules the values compare well with those of McClellan and Harnsberger. Finally, the contribution of these new cross-sectional values to attain a set of coherent quantities from the adsorption experiments is revealed.

Introduction

A quantitative description of the adsorption from liquid solutions by solids includes the determination of concentration profiles as well as molecular orientation and packing over the surface.[1] In fact, the adsorption equilibrium involves drastic changes in the molecular environment, implying the disruption of the solvent cages and the imposition of specific directional adsorbate−surface interactions.[2] This phenomenon has been described by simplified models, which, although not physically realistic, are useful in the correlation and interpretation of experimental adsorption data.[1] Nonetheless, work concerning the correlation of experimental data with molecular shape parameters is scarce, though undoubtedly necessary, for a deeper understanding of such a complex process.[2,3]

Experimental data obtained for the adsorption of triethylamine and tributylamine solutions in toluene onto AgI in the very dilute region were analyzed using Everett's model for the perfect adsorbed monolayer[4] and using Sircar and Myers[5] application of the pore filling model for essentially energetically homogeneous and nonporous and surfaces, like AgI.[6,7] This comparison of Everett's simple and successful model with the Sircar and Myers model, where molecular size differences between adsorbates are contemplated, was chosen to allow a comparative study between systems where there is a symmetric hydrocarbon chain length increase on going from one tertiary amine to the other.

These systems are sensitive to size and shape but also to molecular orientation, since the obvious nonspherical shape of the solvent necessarily leads to difficulties in the calculation of molecular cross sections for this adsorbate, thus screening or eventually canceling the effects due to spherical shape deviations of the other component (tertiary amine). Consequently, the need of cross sections for nonspherical molecules was felt and a method for their calculation presented.

Experimental Section

Materials. Silver iodide was synthesized by a slow addition (2 cm^3 min^{-1}) of equal volumes of a 0.202 M potassium iodide solution to a 0.200 M silver nitrate solution under constant stirring. The precipitate was separated by decantation and thoroughly washed with doubly distilled water until a conductivity identical with the one of the doubly distilled water was obtained for the last wash water. The solid was finally dried for 12−14 h in a vacuum oven at 378 K and under reduced pressure (P < 100 Pa).[6,7] The solid was ground in an agate mortar and the solid particles, which passed through a 70 mesh copper sieve (≤210 μm), were collected and used in the adsorption experiments. Further evacuation of the sieved silver iodide, at room temperature and 10^{-1} Pa for 48 h, proved to be irrelevant in terms of the adsorption measurements.

Samples of independent preparations of silver iodide were characterized by X-ray diffraction and BET specific surface area determinations. The X-ray diffraction spectra of several silver iodide samples showed the solid was polycrystalline and predominantly composed of β-AgI. The lattice parameters for silver iodide were a_0 = 4.5939 Å and c_0 = 7.512 Å, values that deviate less than 0.04% from those published by the Joint Committee for Powder Diffraction Standards (Powder Diffraction File no. 9-374)[8] for the hexagonal structure of this crystalline form of silver iodide. The BET specific surface area of silver iodide, determined by nitrogen adsorption, was 0.407 ± 0.003 m^2 g^{-1}.

Toluene, Aristar grade (purity, ≥99.95%), was supplied by BDH and was used without further purification. The amines, triethylamine (Merck, *p. synthesis* grade) and tributylamine (BDH, gpr grade), were treated with acetic anhydride and fractionally distilled, refluxed over potassium hydroxide, and finally fractionally distilled from barium oxide through a column packed with Pyrex glass rings, as described by Barbosa and Lampreia.[9] Tributylamine was distilled under a reduced pressure of 1 kPa because of the high normal boiling point of this compound. The purity of all liquids was determined by GC, being 99.98% for the solvent toluene, 99.94% for triethylamine, and 99.98% for tributylamine.

Liquid density measurements were also performed and compared with the experimental literature values for these substances to further test the quality of the components used. The densities were measured at 298.150 ± 0.001 K using an

* To whom correspondence should be addressed. Telephone: 351-1-3906138. Fax: 351-1-7500088. E-mail: Ester.Barbosa@fc.ul.pt.

S1089-5647(98)00891-8 CCC: $15.00
Published on Web 07/15/1998

Anton Paar 02D vibrating tube densimeter in the setup previously described by Barbosa and Lampreia.[9] The densimeter was calibrated with doubly distilled water ($\rho = 0.997\,047$ g cm^{-3}) and toluene of known density ($\rho = 0.862\,196$ g cm^{-3}) previously determined in a modified Ostwald picnometer.[10] Densities from different solvent flasks were determined, and the following data resulted in 0.862 126 and 0.862 155 g cm^{-3} values, which deviate less than 0.01% from the data obtained by Letcher[11] and Sousa et al.,[10] as well as less than 0.02% from the data of Garbajosa et al.[12] For triethylamine the experimentally determined density was 0.723 045 g cm^{-3}, a value that falls well within the values obtained by Barbosa and Lampreia[9] ($\rho = 0.723\,01$ g cm^{-3}) and Letcher[11] ($\rho = 0.723\,18$ g cm^{-3}). The density determined for the tributylamine was 0.773 447 g cm^{-3}, a value well within the data published by other authors ($\rho = 0.770\,36$ g cm^{-3}) [9] and ($\rho = 0.77378$ g cm^{-3}) [11] for this amine.

Adsorption Method and Measurements. The adsorption isotherms were obtained by the immersion method,[1] and the composition of the solution in equilibrium with solid was determined by differential refractometry.

Adsorption cells consisted of cylindrical glass vessels with conical glass joint necks closed by Teflon lids with tightly fitting Viton "O" rings.

Adsorption mixtures were prepared by weight in a shaded room by successive addition of solid (2.5−5.0 g) and of dilute amine solution (∼10 mL) to the adsorption cells containing a Teflon magnetic stirrer. The adsorption mixtures were equilibrated in a thermostatic water bath at 298.15 ± 0.05 K under constant stirring at 2500 rpm and below a close-packed superficial layer of polyethylene balls.

The adsorption cells were centrifuged for 10 min at 2000 rpm after direct transfer from the thermostatic bath. The original Teflon lids were then quickly exchanged with new Teflon stoppers fitted with a pair of hypodermic stainless steel needles. A sample of supernatant solution was collected with polyethylene syringes through one of the hypodermic needles and immediately introduced into the sample cell of the refractometer. The equilibrium was established in less than 15 min and was maintained at least for 24 h.

Several adsorption blanks for the solvent toluene were prepared and analyzed. These blanks showed no dependence with respect to identical but independent preparations of solid samples but revealed a small and constant dependence on the solvent flask, which was discounted in the corresponding adsorption measurements.

Special care was taken in the preparation of the dilute solutions used in the adsorption experiments as well as in the calibration curves. Amine solutions in toluene were prepared by weight in adapted volumetric flasks, designed by Barbosa and Lampreia, and according to the procedure developed by these authors for the experimental determination of partial molar volumes in dilute solutions.[9]

The composition of the solutions in equilibrium with the solid was determined using a differential refractometer R401 from Waters Associates and a calibration curve constructed by successive and crossed comparison of pairs of amine solutions of known composition.[13] The reproducibility of the differences between the refractive index of successive solutions (Δn) was improved by connecting the refractometer to a digital multimeter Keithley M197 and by collecting all data for readouts between 0 and 8 mV. A careful selection of the attenuation ranges, and the reduction of all data into an arbitrary scale (Δn_{ap}) lead to a high sensitivity of the refractometer for an extended range of compositions.

The change in the composition of the solutions due to the solid (Δx) was determined from the slope of the calibration curves through direct comparison with a solution of known composition ($\Delta x = \Delta(\Delta n_{ap})$/slope).

Results and Discussion

The refractometric calibration curves of Δn_{ap} versus the mole fraction of the amine solution x_B are linear in the very dilute region studied, namely, $x_B \leq 0.0073$ and $x_B \leq 0.0044$ for triethylamine and tributylamine, respectively. The experimental data points were fitted using linear least-squares fits, and the 34 experimental points used in the triethylamine calibration curve led to the following equation

$$\Delta n_{ap} = (0.3 \pm 0.3) + (13853.5 \pm 83.4)x_B$$

with $\sigma_{fit} = 1$. The calibration curve for the tributylamine solutions was based on the analysis of 23 mixtures and the fitted equation

$$\Delta n_{ap} = (0.07 \pm 0.26) + (20005.1 \pm 45.6)x_B$$

with $\sigma_{fit} = 0.3$. The results of the adsorption experiments for triethylamine and tributylamine solutions in toluene are presented in Tables 1 and 2, respectively. These tables include data obtained using different experimental procedures, namely, different contact times of the adsorbent with the solution and different pretreatments of the adsorbent, as described in the previous section.

The surface excess quantities, defined per unit mass and with respect to a Gibbs dividing surface (GDS) located on the solid surface[1] (specific reduced surface excess quantities) were determined at 298.15 ± 0.05 K using the expression

$$\frac{n_B^{\sigma(n)}}{m} = \frac{n^0 \Delta x_B^l}{m} \qquad (1)$$

where n^0 is the total amount of components A and B in the system, x_B^0 the initial concentration of substance B, and $\Delta x_B^l = x_B^0 - x_B^l$ is the change of the bulk mole fraction of B after equilibration with a mass m of solid.

Equation 1 clearly shows that, above all in the very dilute region, the major factor conditioning the reliability of the specific reduced surface excess isotherms is the quality of the calibration curves used, thus justifying all the care, mentioned in the previous section, put into its attainment. The quality of the fits for both calibration curves and in particular the standard deviation associated with the slope of the plots ascertain the attributes of the experimental isotherms obtained.

The adsorption isotherms for both amines are plotted in Figure 1, and the data clearly show that in both systems the amines are preferentially adsorbed in the concentration range studied. These data also show that the amount adsorbed is lower in the superficial phase containing the bulkier amine. Furthermore, it is clear that the affinity for the surface is larger for the smaller amine.

The interpretation of the adsorption data in terms of molecular orientation and concentration profiles in the vicinity of the surface involves the use of simplifying models to interpret and correlate experimental data.

Models. *Everett Model.* The perfect solution/solid interface is a very simple model, imagined by Everett,[4] which has been

TABLE 1: Specific Surface Excess Isotherm for the Adsorption of Dilute Triethylamine Solutions in Toluene onto AgI at 298 K

contact time, min	x_B^0	n^0	m_{AgI}	$\Delta(\Delta n_{ap})$	x_B^l	$n_B^{\sigma(n)}/m$, mol g^{-1}
1440	1.34×10^{-5}	6.76×10^{-2}	3.3910	−0.13	4.00×10^{-6}	1.87×10^{-7}
30	1.34×10^{-5}	6.76×10^{-2}	3.3880	−0.12	4.72×10^{-6}	1.73×10^{-7} [a]
1200	2.20×10^{-4}	9.56×10^{-2}	3.4212	−0.91	1.55×10^{-4}	1.84×10^{-6}
1440	5.25×10^{-4}	1.25×10^{-1}	3.5061	−1.16	4.41×10^{-4}	2.98×10^{-6}
960	8.28×10^{-4}	6.67×10^{-2}	4.1848	−2.78	6.28×10^{-4}	3.20×10^{-6}
30	8.28×10^{-4}	1.01×10^{-1}	5.4384	−2.55	6.44×10^{-4}	3.42×10^{-6}
1080	8.29×10^{-4}	5.87×10^{-2}	1.8683	−1.51	7.20×10^{-4}	3.43×10^{-6}
1440	1.24×10^{-3}	1.39×10^{-1}	6.4304	−2.51	1.06×10^{-3}	3.92×10^{-6}
1200	1.41×10^{-3}	1.50×10^{-1}	4.2168	−1.52	1.30×10^{-3}	3.92×10^{-6}
1210	1.48×10^{-3}	1.31×10^{-1}	3.1003	−1.32	1.38×10^{-3}	4.03×10^{-6} [a]
30	1.60×10^{-3}	1.33×10^{-1}	3.7170	−1.53	1.49×10^{-3}	3.96×10^{-6}
1440	1.60×10^{-3}	1.40×10^{-1}	3.5866	−1.41	1.50×10^{-3}	3.98×10^{-6}
15	1.68×10^{-3}	1.40×10^{-1}	4.7507	−1.88	1.54×10^{-3}	4.01×10^{-6}
1140	1.70×10^{-3}	1.40×10^{-1}	4.6872	−1.88	1.57×10^{-3}	4.07×10^{-6}
1440	1.68×10^{-3}	1.42×10^{-1}	2.8981	−1.15	1.60×10^{-3}	4.07×10^{-6}
1020	1.68×10^{-3}	1.42×10^{-1}	2.8981	−1.13	1.60×10^{-3}	4.00×10^{-6}
30	1.70×10^{-3}	1.01×10^{-1}	0.8680	−0.48	1.67×10^{-3}	4.10×10^{-6}
1200	1.90×10^{-3}	1.43×10^{-1}	4.0948	−1.59	1.79×10^{-3}	4.04×10^{-6}
1440	2.01×10^{-3}	1.27×10^{-1}	4.4972	−1.94	1.87×10^{-3}	3.98×10^{-6} [a]
1200	2.01×10^{-3}	1.38×10^{-1}	4.2555	−1.74	1.88×10^{-3}	4.09×10^{-6}
1320	2.19×10^{-3}	1.42×10^{-1}	4.7950	−1.90	2.05×10^{-3}	4.07×10^{-6}
1320	2.21×10^{-3}	1.35×10^{-1}	4.2378	−1.79	2.08×10^{-3}	4.13×10^{-6}
1440	2.56×10^{-3}	1.35×10^{-1}	3.5009	−1.47	2.45×10^{-3}	4.10×10^{-6}
1440	2.76×10^{-3}	1.32×10^{-1}	3.5844	−1.58	2.65×10^{-3}	4.24×10^{-6}
1260	3.44×10^{-3}	1.39×10^{-1}	3.7348	−1.58	3.32×10^{-3}	4.26×10^{-6}
1260	4.19×10^{-3}	1.33×10^{-1}	4.1525	−1.82	4.06×10^{-3}	4.24×10^{-6}
1320	4.58×10^{-3}	1.51×10^{-1}	4.7794	−1.83	4.45×10^{-3}	4.17×10^{-6}
1320	4.98×10^{-3}	1.33×10^{-1}	3.9548	−1.76	4.85×10^{-3}	4.30×10^{-6}
1380	5.80×10^{-3}	1.21×10^{-1}	4.4217	−2.19	5.64×10^{-3}	4.35×10^{-6}
1380	5.82×10^{-3}	1.32×10^{-1}	3.8270	−1.72	5.70×10^{-3}	4.34×10^{-6} [a]
1440	5.82×10^{-3}	1.35×10^{-1}	3.7976	−1.66	5.70×10^{-3}	4.34×10^{-6}
1440	6.58×10^{-3}	1.36×10^{-1}	4.7525	−2.06	6.43×10^{-3}	4.29×10^{-6}

[a] Adsorbent further degassed in the adsorption cell, after grinding, at room temperature at 10^{-1} Pa for 48 h.

TABLE 2: Specific Surface Excess Isotherm for the Adsorption of Dilute Tributylamine Solutions in Toluene onto AgI at 298 K

contact time, min	x_B^0	n^0	m_{AgI}	$\Delta(\Delta n_{ap})$	x_B^l	$n_B^{\sigma(n)}/m$, mol g^{-1}
1200	5.44×10^{-5}	1.19×10^{-1}	3.3100	0.24	3.98×10^{-5}	5.29×10^{-7}
1230	1.08×10^{-4}	1.12×10^{-1}	2.8793	0.08	8.49×10^{-5}	8.80×10^{-7}
1440	1.58×10^{-4}	1.18×10^{-1}	3.4644	−0.13	1.25×10^{-4}	1.13×10^{-6}
1440	1.75×10^{-4}	1.10×10^{-1}	3.1386	−0.17	1.40×10^{-4}	1.23×10^{-6}
15	3.26×10^{-4}	9.13×10^{-2}	4.2720	−1.10	2.45×10^{-4}	1.74×10^{-6}
30	3.26×10^{-4}	9.20×10^{-2}	4.0394	−1.10	2.45×10^{-4}	1.86×10^{-6}
1440	3.26×10^{-4}	1.10×10^{-1}	4.9679	−1.06	2.47×10^{-4}	1.76×10^{-6}
1440	5.23×10^{-4}	1.18×10^{-1}	4.2704	−0.98	4.48×10^{-4}	2.09×10^{-6}
30	7.98×10^{-4}	9.96×10^{-2}	2.6147	−0.75	7.34×10^{-4}	2.44×10^{-6}
1440	8.23×10^{-4}	1.15×10^{-1}	4.3684	−1.25	7.34×10^{-4}	2.35×10^{-6}
1020	7.98×10^{-4}	9.60×10^{-2}	2.6057	−0.72	7.35×10^{-4}	2.31×10^{-6}
1440	9.51×10^{-4}	1.13×10^{-1}	4.0471	−1.21	8.64×10^{-4}	2.44×10^{-6} [a]
15	9.51×10^{-4}	1.13×10^{-1}	3.5108	−1.02	8.73×10^{-4}	2.50×10^{-6}
1320	1.16×10^{-3}	9.42×10^{-2}	3.4404	−1.35	1.06×10^{-3}	2.58×10^{-6}
1320	1.31×10^{-3}	1.12×10^{-1}	2.9160	−0.83	1.24×10^{-3}	2.61×10^{-6}
30	1.52×10^{-3}	9.22×10^{-2}	5.5636	−2.86	1.35×10^{-3}	2.81×10^{-6} [a]
1140	1.52×10^{-3}	9.59×10^{-2}	5.5635	−2.58	1.37×10^{-3}	2.68×10^{-6} [a]
1440	1.52×10^{-3}	1.01×10^{-1}	4.0329	−1.68	1.41×10^{-3}	2.76×10^{-6}
30	1.78×10^{-3}	9.13×10^{-2}	4.0334	−1.91	1.66×10^{-3}	2.77×10^{-6}
1320	2.17×10^{-3}	1.06×10^{-1}	3.5484	−1.29	2.07×10^{-3}	2.72×10^{-6}
1440	3.74×10^{-3}	9.35×10^{-2}	3.4596	−1.61	3.63×10^{-3}	2.90×10^{-6} [a]
1440	3.74×10^{-3}	1.03×10^{-1}	3.0389	−1.16	3.65×10^{-3}	2.86×10^{-6}
1440	4.41×10^{-3}	9.05×10^{-2}	2.7350	−1.32	4.32×10^{-3}	3.06×10^{-6}

[a] Adsorbent further degassed in the adsorption cell, after grinding, at room temperature at 10^{-1} Pa for 48 h.

very successful in the interpretation of adsorption data, as well as the calculation of the surface area of solids.

According to the model of the perfect adsorbed monolayer, the preferential adsorption of a component from a binary liquid mixture of substances with approximately the same size is supposed to be monomolecular. The set of adsorbed molecules, immediately adjacent to the solid surface, occupying identical surface sites constitute the adsorbed phase, which has a composition different from that of the bulk solution. Under these assumptions and choosing a GDS at the solid surface,[1] Everett was able to relate experimentally determined quantities (Δx_B^l) to the reduced surface excess ($n_B^{\sigma(n)}$) using eq 2:

$$\frac{n_B^{\sigma(n)}}{m} = \frac{n^0 \Delta x_B^l}{m} = \frac{n_m^s x_A^l x_B^l (S-1)}{m(S x_B^l + x_A^l)} \qquad (2)$$

where x_A^l and x_B^l refer to the solvent and solute mole fraction in

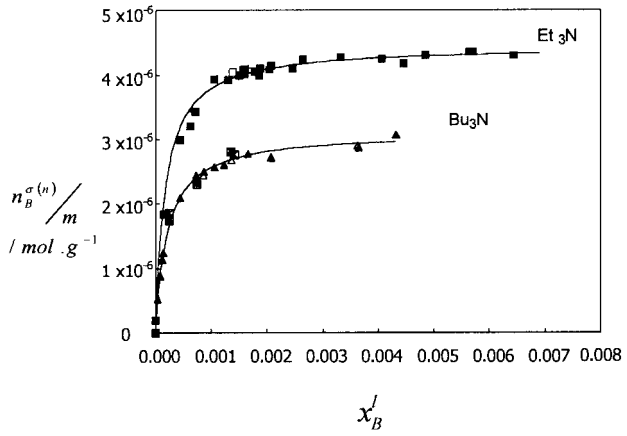

Figure 1. Experimental specific surface excess isotherms for the adsorption of dilute triethylamine and tributylamine solutions in toluene onto AgI at 298 K.

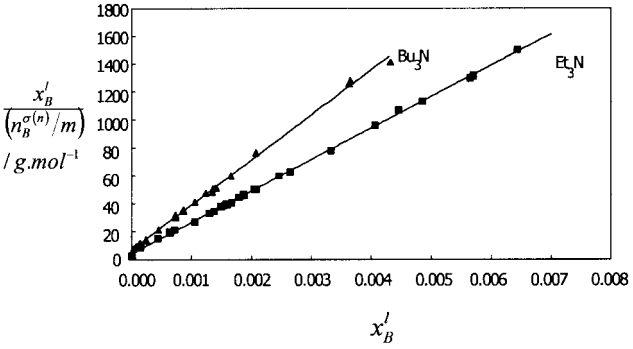

Figure 2. Plots of the linearized form of Everett equation (eq 3) for the adsorption of triethylamine and tributylamine solutions in toluene onto AgI at 298 K.

the liquid phase respectively, n_m^s is the number of moles in the monomolecular adsorbed phase, and *S*, the separation factor, is the equilibrium constant for the exchange reaction between the uniform monomolecular adsorbed phase and the liquid phase ($S = x_B^s x_A^l/(x_A^s x_B^l)$).

In the very dilute region, $x_A^l \approx 1$ and eq 2 can be approximated by the linear equation

$$\frac{x_B^l}{n_B^{\sigma(n)}/m} = \frac{m x_B^l}{n_m^s} + \frac{m}{n_m^s(S-1)} \tag{3}$$

which enables the calculation of both quantities (*S* and n_m^s) directly from the slope and intercept of the linear plot of $x_B^l/(n_B^{\sigma(n)}/m)$ as a function of x_B^l (Figure 2).

Further checking of the validity of eq 3 involved a nonlinear fit of eq 2 to the experimental data. This fit was done using a Marquardt−Levenberg algorithm[14,15] and introducing the values obtained above for *S* and n_m^s as preliminary estimates for these quantities. Convergence was attained in less than 13 iterations and led to values identical with the ones derived previously from the application of eq 3, thus showing that the approximation is valid in the concentration range studied.

Table 3 presents the calculated equilibrium constant for adsorption and the amount in the adsorbed phase obtained by the least-squares fit of eq 3, since the error estimates are more reliable for this method.

The equilibrium constants for the exchange process between solution and adsorbed phase are calculated indirectly by a ratio of the slope over the intercept and consequently exhibit relatively high uncertainties. Nonetheless these values make evident the extremely high affinity of the adsorbate (amine) for the surface. This high affinity is associated with strong acid−base interactions between the surface and the amines. The data also display the decrease in basicity associated with the increase of the alkyl chains of the amines.

On the other hand the number of amine molecules in a filled monolayer, n_m^s, is calculated directly by the slope of eq 3, so it is very precise. These quantities make evident the expected effect of going from the smaller to the bulkier amine.

If the assumptions of the model are correct, the specific surface area for the solid (a_s) can be calculated by resorting to the areas per molecule of both amines according to the following equation

$$a_s = \frac{a_{m,i} n_m^s L}{10^{20} m} \tag{4}$$

where $a_{m,i}$ is the area per molecule in a filled monolayer (in square angstroms) and *L* is Avogadro's number.

At this stage the widely known eq 5, reported by McClellan and Harnsberger,[17]

$$a_{m,i}^{Mc-H} = 1.091\left(\frac{M}{L\rho_i}\right)^{2/3} \times 10^{16} \approx \frac{\pi}{0.9069}(0.74)^{2/3}\left(\frac{3}{4\pi}\right)^{2/3}\left(\frac{M}{L\rho_i}\right)^{2/3} \tag{5}$$

where *M* is the molecular weight and ρ_i is the liquid density (in grams per cubic centimeter) at the temperature of adsorption, will be used. This equation relies on the assumption of a condensed phase composed by spherical molecules with a hexagonal close-packed arrangement over a bidimensional surface[16,17] and will be used to calculate the molecular cross-sectional area ($a_{m,i}^{Mc-H}$) from the liquid density.

The experimentally determined solvent and solute densities at the temperature of adsorption allowed the calculation of the molecular cross sections for triethylamine (41.2 Å^2) and for tributylamine (59.0 Å^2). Consequently, the specific surface areas calculated for the samples of β-AgI prepared are 1.09 and 1.08 m^2 g^{-1}, respectively.

These values for the specific surface area of AgI samples lie well within those determined by independent wet methods (negative adsorption, capacitance, and dye adsorption) by van den Hull and Lyklema[7] for several AgI samples, namely, 0.81 and 1.6 m^2 g^{-1}. A comparison of the specific surface areas determined by dry and wet methods for the synthesized β-AgI in this work, namely, BET and solution/solid adsorption, shows a ratio of $^1/_{2.6}$. This relation is identical with the one reported by van den Hull and Lyklema,[7] authors who found consistently and repeatedly factors varying between 2 and 3 for the ratio of wet to dry specific surface areas (gas adsorption, air permeability, and electron microscopy) for identical samples of AgI. This systematic decrease of the specific surface area, determined by dry methods, was attributed to reversible aggregation phenomena occurring during the solid drying process,[7] an aggregation that was also observed in the electron micrographs of dry samples of β-AgI synthesized in this work.

Everett's model of the ideal adsorbed monolayer, employed throughout this section, may be extended to nonideal adsorption. Several expressions have been proposed for the specific reduced surface excess isotherms of binary nonideal liquid mixtures of molecules of unequal size on energetically homogeneous

TABLE 3: Parameters Estimated by Eqs 3 and 6 from Specific Surface Excess Isotherms of Dilute Triethylamine and Tributylamine Solutions in Toluene at 298 K

	Everett eq 3		Sircar and Myers eq 6						
			spherical molecules			this work			
amines	$(n_s^m/m \pm \sigma) \times 10^6$, mol g^{-1}	$(S \pm \sigma) \times 10^{-3}$	S_0	$(n_s^m/m \pm \sigma) \times 10^6$, mol g^{-1}	β (Mc-H)	$(n_s^m/m \pm \sigma) \times 10^6$, mol g^{-1}	β, barrel toluene spherical amines	$(n_s^m/m \pm \sigma) \times 10^6$, mol g^{-1}	β, barrel toluene barrel amines
Et_3N	$4.4_4 \pm 0.02$	$5._7 \pm 1$	5726	$4._6 \pm 0.08$	0.835	$4.4_1 \pm 0.02$	1.060	$4.4_4 \pm 0.02$	1.014
Bu_3N (all data)	$3.1_1 \pm 0.03$	$4._7 \pm 0.5$	4708	$3._6 \pm 0.09^a$	0.584	$3._4 \pm 0.07^b$	0.736	$3._4 \pm 0.07^b$	0.735
Bu_3N ($0.00014 \leq x_{Bu_3N} \leq 0.0044$)			4708	$3._7 \pm 0.2^c$	0.584	$3.2_1 \pm 0.02^d$	0.736	$3.2_1 \pm 0.02^d$	0.735

[a] Intercept $= (-2._5 \pm 0.6) \times 10^{-7}$. [b] Intercept $= (-1._2 \pm 0.5) \times 10^{-7}$. [c] Intercept $= (-3 \pm 1) \times 10^{-7}$. [d] Intercept $= 0$.

adsorbents.[5,18,19] The approach elected by us was that of Sircar and Myers and is presented below.

Sircar and Myers Model. For nonporous solids,[19] such as AgI,[6,7] the Sircar and Myers[5,19] monolayer-pore filling model for the adsorption isotherms of binary liquid mixtures of different sizes takes the form of eq 6:

$$\frac{n_B^{\sigma(n)}}{m} = \frac{n_m^s (S a_B^l x_A^l - a_A^l x_B^l)}{m(S a_B^l + \beta a_A^l)} \tag{6}$$

where S is composition-dependent and changes according to equation

$$S = S_0 (S a_B^l + a_A^l)^{\beta - 1/\beta} \tag{7}$$

whenever the adsorbates have different sizes and where S_0 is the value of S at infinite dilution, a_A^l and a_B^l are the solvent and solute activities in solution, respectively. β ($=a_{m,A}/a_{m,B}$) is the ratio of the areas per molecule of the solvent ($a_{m,A}$) and the solute ($a_{m,B}$). At this point we made use of eq 5 to calculate the molecular cross sections ($a_{m,i} = a_{m,i}^{Mc-H}$).

The varying S values were calculated by successive iterations on eq 7 (taking $a_i = x_i$ for both components) until a 0.1% convergence was attained, beginning with the introduction of the S_0 value estimated by the perfect adsorbed monolayer (S).

The calculation of the amount adsorbed per gram of adsorbent, n_m^s/m, by means of eq 6 may then be accomplished by plotting the specific reduced surface excess as a function of the factor

$$\frac{S a_B x_A^l - a_A x_B^l}{S a_B + \beta a_A}$$

This representation, presented in Figures 3 and 4, should be linear and go through the origin if the model as well as the assumptions underlying its application is correct.

The linear least-squares fits corresponding to the plot of function 6 lead to poor fits for both amines, showing systematic and extremely high residuals (up to 35%) in the low concentration regions ($x \leq 0.00014$) and indicating a tendency toward improvement upon increase of β values. These data, presented in Table 3, disclosed the need for a deeper analysis of the model and its application, in particular for the bulkier amine, where deviations from the expected plots are evident (Figures 3 and 4). A debatable step, underlying the application of the Sircar and Myers model, is the calculation of the area per molecule ($\beta = a_{m,A}/a_{m,B}$).

For the systems reported here, there is a clear deviation from sphericity for at least one of the components (toluene), apart from the strong specific surface−adsorbate interactions,[20−22]

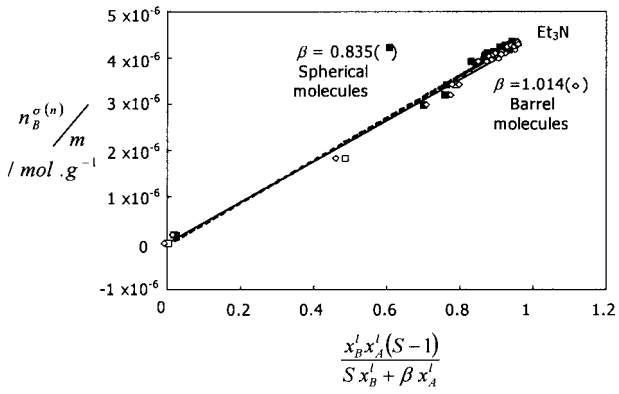

Figure 3. Sircar and Myers plots (eq 6) for the adsorption of dilute triethylamine solutions in toluene onto AgI at 298 K for different β values calculated by considering molecules to be either spherical or barrel-type.

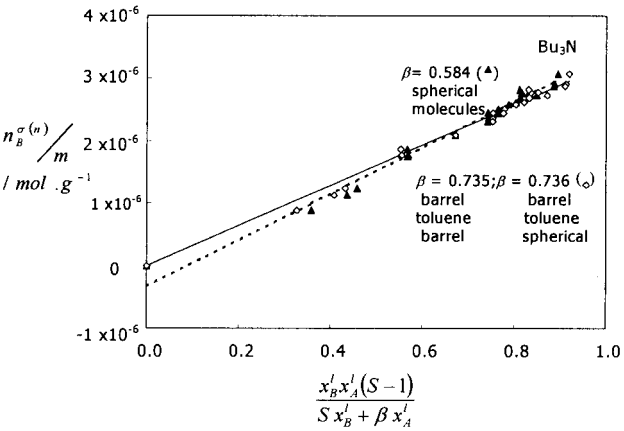

Figure 4. Sircar and Myers plots (eq 6) for the adsorption of dilute tributylamine solutions in toluene onto AgI at 298 K for different β values calculated by considering molecules to be either spherical or barrel-type.

which may impose conformational constraints on the molecules in the adsorbed phase. These limitations prompted a reconsideration of the molecular cross-section estimates, bearing in mind molecular shape and orientation over the solid surface.

Adsorbed Phase: Estimation of Cross-Sectional Areas. Adsorption is associated with donor−acceptor interactions between the adsorbate and the surface. According to Farin et al.[3] and Meyer et al.,[2,23−25] a molecular approach should be used to determine molecular orientations and cross sections in the adsorbed phase in order to undertake a correct analysis of adsorption data. In fact, during the adsorption process the adsorbate is involved in exchange equilibrium with the liquid phase, while simultaneously, only specific moieties of the adsorbate are exposed and block the adsorbent surface. So,

addressing the adsorbed phase in terms of molecular models for both components can provide additional awareness in the choice of adsorption models and of the interpretation of experimental data, as molecular cross sections for all orthogonal planes can be calculated and considered.

Meyer's Procedure. Meyer et al.[2,23−25] introduced the concept of reduced molecular (rm) bodies to represent the molecules and to allow the calculation of molecular properties, namely, volume, surface area, and cross sections.

According to Meyer,[2,23−25] molecules are depicted as expanded van der Waals bodies (rm bodies) with a volume V_{rm} close but smaller than the molar volume (V_m). These reduced molecular bodies have their shape defined by the interlocking of spheres of adequate radii, as in the van der Waals approach, and the enlargement of the molecular volume is accomplished through an increase of the radii for the denominated "mantle"[2,25] atoms. This process of building up a bulk volume from rm solids, with well-defined shapes other than parallelepipeds, leaves interstitial holes with a volume that cannot be estimated ($V_{rm} \cong V_m$).

In this type of approach "core" atoms define molecular shape, but properties such as molar volume or molar surface area are determined by the molecular envelope defined by the rm body and can be calculated from the reduced molecular radii of mantle atoms.

This laborious procedure is extremely powerful and allows the calculations of molecular cross sections for every specific conform of a molecule along any plane ($a_{m,i}^{rm,xy}$; $a_{m,i}^{rm,xz}$; $a_{m,i}^{rm,yz}$) for the rm bodies.

The values obtained for specific molecular orientations correlate well with adsorption measurements, thus providing a valuable tool in the prediction of orientation for adsorbed species.[2] Such satisfactory correlation means that the adsorbed molecules orient themselves in such a way that no holes are left between next neighbors and the expression for the area of the surface (A)

$$A = Ln_{m,N_2}^{\sigma} a_{m,N_2} = Ln_{m,B}^{\sigma}\, a_{m,B}^{rm} \qquad (8)$$

is applicable, or that the differences in the packing efficiency factors over surfaces for different molecular shapes are very small ($a_{m,N_2}/a_{m,B} \approx a_{m,N_2}^{rm}/a_{m,B}^{rm}$), or even both. Consequently, any area (A) estimated exclusively in terms of molecular cross sections of rm bodies will be overestimated by the area of the equivalent volume cuboid,[24,25] since the molecular voids generated by molecular packing are ignored in such a procedure.

For the systems reported here, apart from the rigidity of the aromatic ring of toluene and its polarizibility, which determine the effective molecular cross-sectional area over a polarizing surface, a small distortion of amine molecules is expected upon adsorption. The complexity underlying Meyer's analysis of these systems leads us to try to develop a simpler procedure to improve estimates for the molecular cross-sectional areas of adsorbed molecules when compared with the spherical approximation, contemplating molecular shape and orientation in terms of average geometrical solids.

This Work. A new procedure that tries to account for molecular shape and superficial orientation over a surface is proposed, and which is based on the application of solution partial molar volumes semiempirical theories to the experimentally determined solvent and solute densities.

In this approach molecular shape is approximated by simple geometrical shapes, like the spherocylinder or the barrel,[26] and the molecular volume is seen as composed of an intrinsic volume, defined by the van der Waals volume according to Bondi,[27] and a void volume symmetrically distributed over all molecular dimensions.

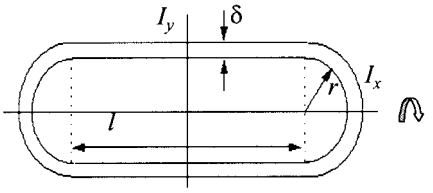

Figure 5. Schematic representation of spherocylinder-type molecules, including the identification of symmetry axes (XX', YY') according to Meyer.

Such a procedure develops from Kharakoz's[26] semiempirical approach to solution partial molar volumes, where molecular shape dependencies were introduced. In the present study the adsorbed monolayer on a particular solid was considered a pure liquid, making possible the application of Kharakoz's volumetric reasoning to the interfacial region. Since molecular orientations on a surface are conditioned by the specific adsorptive-surface interactions for simple geometrical shapes, the calculation of cross-sectional areas for all possible projections in the adsorbed phase for solvent and solute in the most appropriate position was possible and straightforward.

Taking the general form for the molar volume at infinite dilution of a solute B ($\bar{V}_B^0$)

$$\bar{V}_B^0 = \bar{V}_{cav} + \bar{V}_i + \kappa_T RT \qquad (9)$$

where $\bar{V}_{cav}$ is the molar volume of the cavity large enough to accommodate the solute and can be estimated theoretically for spherical molecules by the scaled particle theory (SPT), $\bar{V}_i$ is the interaction volume, which measures the volume increment associated with solute−solvent interactions (for pure substances taken as $\bar{V}_i = 0$ [9]), and $\kappa_T RT$ accounts for the change in standard state between gas and solution. Kharakoz[26] considered that the cavity volume was composed of the hard core molecular volume of a particular shape plus a void volume of constant thickness (δ) around the solute, which is characteristic of the solvent but independent of solute shape. Since $\bar{V}_{cav}$ may be calculated from experimental partial molar volumes at infinite dilution, provided interaction volumes and isothermal compressibilities are known, the empty thickness (δ) may then be evaluated.

The approach employed in this work was comparatively tested, in a first instance, with the data for alkanoic acids reported by Meyer et al.[2] These molecules were approximated by a spherocylinder schematically presented in Figure 5.

The cavity volume for a spherocylinder is given by eq 10

$$\bar{V}_{cav} = \left(\frac{4\pi N_A}{3}\right)(r+\delta)^3 + \pi N_A l (r+\delta)^2 \qquad (10)$$

where r is the radius of the cylinder that approximates the long straight aliphatic chain, l the corresponding internal length, and δ the empty thickness mentioned above. The hard core volume calculated after Bondi was equated to

$$\bar{V}_w = \left(\frac{4\pi N_A}{3}\right) r^3 + \pi N_A l r^2 \qquad (11)$$

The length of the alkanoic acids $l_{CH_3(CH_2)_nCOOH}$ was estimated by the length of the corresponding linear hydrocarbon[26] and derived according to eq 12:

$$l_{CH_3(CH_2)_nCOOH} \approx l_{CH_3(CH_2)_nCH_3} = 1.57 + n(1.27)\ \text{Å} \quad (12)$$

Experimental molar volumes and estimates for the isothermal compressibility for these acids yielded the empty thicknesses (δ). (The isothermal compressibilities for the alkanoic acids were estimated on the basis of the value for acetic acid[28a] and considering a dependence of κ_T on the number of carbons of the alkyl chain identical with the one evidenced by straight-chain alcohols.[29])

Finally, the projections on the three orthogonal planes were calculated and are presented in Figure 6 together with the cross-sectional areas obtained by Meyer et al.[3] for the same compounds.

At this point it is worth remarking that this approach, as well as Meyer's, overestimates molecular cross sections, since the interstitial voids associated with molecular packing are not taken into account.

These data suggest that, despite the underlying approximations, the approach proposed leads to results that correlate well with the cross-sectional areas estimated by Meyer et al.[2] in terms of the various projections and, consequently, with the adsorption measurements. So the simple analysis proposed here seems extremely powerful in terms of foreseeing the effect of chain length and, consequently, in the prediction of molecular orientation on surfaces, at least for molecules that can be described approximately by simple smooth enveloping shapes.

The application of this semiempirical approach to any system under study depends above all on the choice of an adequate average molecular shape. In respect to the toluene−trialkylamine mixtures studied in this work and starting with toluene, the barrel shape was chosen (Figure 7) as the most adequate.

1. Toluene. For barrel-type molecules the cavity volume should be equated to

$$\bar{V}_{cav} = \left(\frac{4\pi N_A}{3}\right)(r+\delta)^3 + \pi^2 N_A R(r+\delta)^2 + 2\pi N_A R^2(r+\delta) \quad (13)$$

This equation allows the estimation of the empty thickness (δ) after resorting to Bondi's van der Waals volume for the calculation of the radii (R) for the internal cylinder or half the barrel thickness (r), depending on which of these parameters is introduced as fixed. In this case r was chosen as the fixed parameter because accurate experimental data are available for half the thickness of the benzene aromatic ring (1.77 Å),[26,27] thus providing a good estimate for the toluene molecule. The radius R for the internal cylinder and the empty thickness δ are, respectively, 1.56 and 0.57 Å and were obtained using a $\bar{V}_{cav}$ calculated from the experimental molar volumes, the isothermal compressibility,[28b] and $\bar{V}_i = 0$.

The hypothesis, $r = 1.77$ Å, is probably an underestimation of the barrel thickness, since the volume increase associated with the introduction of the methyl group will render changes in all the dimensions of the barrel. In fact, the additional methyl group induces further loosening and delocalization of the π-ring; however, a concomitant and opposite effect results from the destruction of the right-angle arrangement of liquid benzene, evident in terms of the liquid structure,[30] thus increasing the reliability of the estimated void volume.

Finally, the area per molecule may be calculated by taking into consideration the toluene−AgI donor−acceptor interactions. These interactions enable the prediction of a toluene superficial monolayer composed of molecules sitting side by side with the aromatic cloud parallel to the AgI polarizing surface. The effective radius for the adsorbed toluene aromatic rings corresponds to the sum hard core ($R + r$) + void (δ) and allows the calculation of a molecular cross-sectional area of 47.8 Å^2 for the *XY* projection of the toluene barrel. This estimate, for the area per molecule, is likely to be very reliable in particular for molecules with rigid and unequivocal geometrical shapes and a disordered liquid structure like toluene.

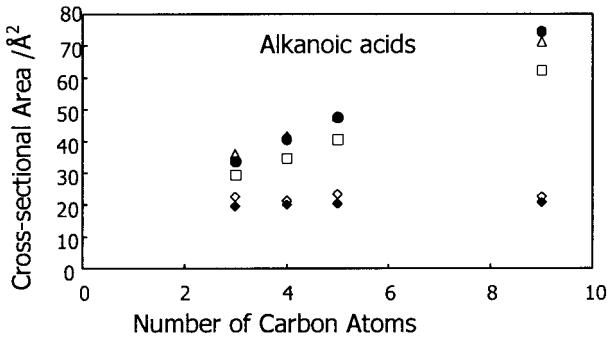

Figure 6. Dependence of calculated cross-sectional areas on the number of carbon atoms for alkanoic acids according to Meyer's and this work's procedure: (△, □) Meyer's values for $a^{xy}_{m,rm}$ and $a^{xz}_{m,rm}$, respectively; (●) this work, $a^{xy}_m = a^{xz}_m$; (◇) Meyer's values for $a^{yz}_{m,rm}$; (◆) this work, a^{yz}_m.

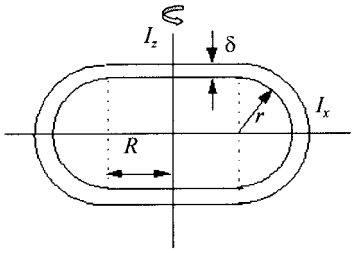

Figure 7. Schematic representation of barrel-type molecules, including the identification of symmetry axes (*XX′*, *ZZ′*) according to Meyer.

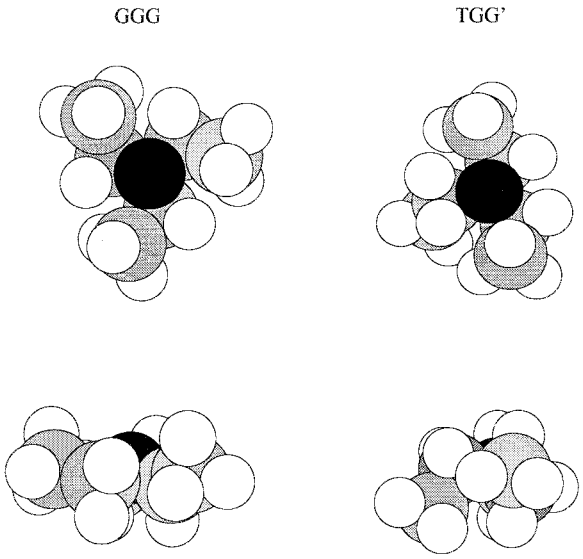

Figure 8. Molecular perspectives for the most symmetrical and asymmetrical conformations of triethylamine along two normal planes.

2. Amines. Turning back to the second components of the systems reported in this work, it must be born in mind that amine adsorption has been attributed to Lewis acid−base interactions between the amine lone electron pair and the surface acid sites.[20−22] Consequently, the preferential adsorption of tertiary amines from toluene solutions onto AgI may be envisaged as the replacement of an attractive solute−solvent interaction by a stronger surface−adsorbate Lewis acid−base attractive inter-

TABLE 4: Effect of the Introduction of Shape Dependency on the Calculation of Molecular Cross-Sectional Areas from Volumetric Data

			this work			
molecule	$V^*_{m,B} \pm \sigma$ $cm^3\ mol^{-1}$	eq 5, $a^{Mc-H}_{m,B}$ $Å^2$	$a_{m,B}$, $Å^2$ (spherical)	$a_{m,B}$, $Å^2$ (spherical)	$a^{xy}_{m,B}$, $Å^2$ (barrel)	$a^{xy}_{m,B}$, $Å^2$ (barrel)
toluene	$106.87_7 \pm 0.004$	34.4			47.8	44.5;[a] 45.8[b]
triethylamine	$139.87_2 \pm 0.001$	41.2	45.1	40.7[a]	47.1	42.6;[a] 44.1[b]
tributylamine	$239.64_9 \pm 0.001$	59.0	64.9	58.7[a]	65.0	58.6;[a] 60.6[b]

[a] Values calculated using a packing efficiency of 0.74 for the tridimensional arrangement of molecules (spheres).[16] [b] Values calculated using a packing efficiency of 0.78 for the tridimensional arrangement of molecules (cylinders).[25]

action. This process imposes directional cleavages on the liquid-phase solvent cages and eventually leads to solute conformational rearrangements, with the corresponding changes in molar volume and cross-sectional areas accompanying the transference of amine molecules from solution to the adsorbed phase.

The extremely high separation factors (S) calculated by the Everett model suggest an adsorbed phase predominantly composed of solute molecules sitting side by side. So the molar volume of the amine, in the superficial monolayer, will be fairly well estimated by its liquid density except if there are significant volume changes upon adsorption, inherent to changes in the overall conformers energetic distribution associated with the specific surface−adsorbate interactions.

For tertiary amines, with identical alkyl chains, shape deviations from molecular sphericity are likely to be small, since the statistically most frequent conformations will be derived from the GGG, TGG, and TGG′ conformations relative to the nitrogen lone electron pair.[31,32] Figure 8 presents two molecular perspectives of triethylamine along normal planes for the most symmetric (GGG) and most asymmetric conformation (TGG′), indicating that the average molecular shape is likely to be a slightly flattened sphere.

In the first stage, the simplest hypothesis was considered; the amine molecules were taken as spherical, a hypothesis that does not seem to be very far from reality based on the molecular models analysis, and the calculations reduced themselves to the determination of the effective radius ($r + \delta$) for both amines. Following the steps already exposed previously in this work $\bar{V}_{cav}$ (Et_3N) for the spherical body was taken from $(M/(L\rho) - \kappa_T RT)$, with $\kappa_T = 10.95 \times 10^{-4}\ MPa^{-1}$ (a value estimated from κ_S and ρ data),[33,34] and for tributylamine a cavity volume of 236.93 $cm^3\ mol^{-1}$ was obtained using the same isothermal compressibility, since no experimental data were available for this amine.

The calculated molecular cross-sectional areas for the amines taken as spherical are 45.1 $Å^2$ for triethylamine and 64.9 $Å^2$ for tributylamine, values that are an overestimation of the true values because of the fact that no void space was considered between molecules. The introduction of the packing efficiency factors for the hexagonal close packing of spheres on tridimensional volumes[16] results in smaller volumes for the hard-sphere spherical bodies values that, when coupled with the appropriate packing factor for circles over bidimensional surfaces, lead to areas per molecule of 40.9 and 58.9 $Å^2$, respectively, for triethylamine and tributylamine. These values compare well with the McClellan and Harnsberger ones (Table 4) and on the other hand reveal the significance of the packing efficiency factors in the condensed phases whenever molecular cross sections are to be used as absolute values.

Further improvement of the model for the tertiary amines implies considering eventual stereochemical constraints due to adsorption. A deeper molecular model conformational analysis allowed us to predict that there are no stereochemical constraints for triethylamine upon adsorption; however, steric constraints were foreseen for the adsorption of all gauche conformations of tributylamine except those derived from the tripropylamine (GT)(GT)(GT), (TT)(GT)(GT), and (TT)(GT)(G′T) conformers.[32] Consequently, it may be concluded that for these symmetrical straight-chain aliphatic amines, the surface influences predominantly the higher energy conformers and have a small effect on the overall conformer equilibrium when compared with the corresponding equilibrium in the liquid phase. Consequently, any improvement of the molecular model for the amines involves considering these molecules more appropriately represented by flattened spheres or barrels (Figure 7).

A critical observation of the molecular models for the most frequent conformers leads us to introduce as a fixed parameter the distance estimated in terms of van der Waals radii, bond distances, and angular projections along the shortest direction. Thus, for triethylamine the barrel thickness r was calculated according to expression 14:

$$r = \frac{1}{2}[r_W(H) + l(C-H) + l(N-C)\sin 14° + l(C-C) + l(C-H)\sin 14° + r_W(H)] \quad (14)$$

and yielded the value $r = 2.82_6$ Å. $R = 0.37$ Å and $\delta = 0.68$ Å were then obtained for this amine. An identical reasoning lead to the introduction of $r = 3.78_3$ Å for tributylamine, and the following values were derived for $R = 0.01$ Å and $\delta = 0.75$ Å. It is worth mentioning that the extremely low values for the calculated R values with respect to r reflect the small deviations from sphericity of these tertiary amines with identical alkyl chains, in particular for the bulkier amine (tributylamine).

Bearing in mind, once more, the specific amine−AgI interactions, which lead to the expectation of barrel-type amine molecules lying flat over the surface, with the nitrogen atom in the center and pointing toward the solid, the molecular projections on the designated XY plane can be calculated. These molecular cross sections, on the XY plane for the amine barrel molecules of volume V ($V = M/(L\rho) - \kappa_T RT$) are presented in Table 4. The table also contains data taking into account estimated molecular packing efficiencies.

Adsorption Models: A Reanalysis. The results for the reexamination of the experimental reduced specific surface excess isotherms in terms of the Sircar and Myers model,[20,21] taking into account the molecular cross sections, as calculated in the previous section were introduced in Table 3. β values (ratio of solvent to solute cross-sectional area) are extremely dependent on the introduction of shape dependency, particularly for toluene, leading to an immediate agreement of the model for both solutes and all the data. Smaller additional deviations from sphericity of the amine do not lead to significant changes either on the quality of the fits to the model or in terms of the estimates for the amount adsorbed.

The data also evidence the fit capacity of Everett's equation, a feature likely to come from the extra degree of freedom on

going from eq 6 to eq 3, clearly screening small deviations of β from unity. The amount adsorbed per mass of adsorbent calculated by means of eqs 3 and 6 is identical, within a 95% confidence interval, for all its estimates in the triethylamine + toluene system ($\beta \approx 1.0$), while for the tributylamine + toluene mixture, where size differences are larger ($\beta \approx 0.7$), this is not so. In fact, if sphericity for both components is heeded, the experimental data points do not obey eq 6 for this latter system. However, upon the introduction of shape dependency for the solvent, all the experimental data conform to the Sircar and Myers model except in the very dilute region ($x_{Bu_3N} \leq 0.00014$) where there is a reduced experimental accuracy.

The quality of the fits for this experimental data set, taking into account molecular shape, further reinforces the reliability of the estimates obtained, apart from corroborating Meyer's hypothesis[25] of relatively small differences in packing efficiency factors for different shapes.

Conclusions

Both systems studied exhibited Langmuir-type adsorption isotherms. The monolayer capacities and separation factors were determined using Everett, and Sircar and Myers models. The deviation from sphericity of toluene and to a lesser extent of the amines prompted the investigation of the adsorption behavior of these mixtures at the molecular level. The extremely accurate and successful description of the adsorption phenomena in terms of molecular models and its projections, developed by Avnir et al.[3] and Meyer et al.,[2,23−25] is very laborious for a quick analysis of the experimental data. A simpler, less accurate but potent tool is proposed in this work. This new procedure allows the analysis of adsorption data for systems containing nonspherical molecules with well-defined molecular envelopes, apart from giving immediate information about the orientation of adsorbed molecules without resorting to elaborate spectroscopic or computational facilities.

This new approach was tested and compared successfully with the data obtained by Meyer et al.'s[2,23−25] rm bodies for alkanoic acids[2] and finally applied to the systems reported here. For spherical molecules, the results were confronted with the widely used McClellan and Harnsberger equation and again good agreement was observed as well.

It is believed that the method here described may constitute a simple and powerful tool in the analysis of adsorption data, where molecular shape, orientation, and void volume are accounted for. It must be also stressed that apart from the parallelism in terms of the estimated cross sections for nonspherical molecules, this approach also indicates the differences in packing efficiencies between aliphatic and aromatic compounds mentioned by Meyer,[25] a quantity measured in this work by the parameter empty thickness.

References and Notes

(1) Everett, D. H. *Pure Appl. Chem.* **1986**, *58*, 967−984.

(2) Meyer, A. Y.; Farin, D.; Avnir, D. *J. Am. Chem. Soc.* **1986**, *108*, 7897−7895.

(3) Farin, D.; Volpert, A.; Avnir, D. *J. Am. Chem. Soc.* **1985**, *107*, 3368−3370.

(4) Everett, D. H. *Trans. Faraday Soc.* **1964**, *60*, 1803−1813.

(5) Sircar, S.; Myers, A. L. *Chem. Eng. Sci.* **1988**, *43*, 3259−3263.

(6) Sidebottom, E. W.; House, W. A.; Jaycock, M. *J. Chem. Soc., Faraday Trans. 1* **1976**, *72*, 2709−2721.

(7) Van den Hull, H. J.; Lyklema, J. *J. Am. Chem. Soc.* **1968**, *90*, 3010−3015.

(8) Klug, H. P.; Alexander, L. E. *X-Ray Diffraction Procedures, for Polycrystalline and Amorphous Materials*, 2nd ed.; John Wiley & Sons: London, 1974; No. 9-374, p 523.

(9) Barbosa, E. F. G.; Lampreia, I. M. S. *Can. J. Chem.* **1986**, *64*, 387−393.

(10) Sousa, S. C.; Barbosa, E. F. G. Personal communication.

(11) Letcher, M. *J. Chem. Thermodyn.* **1972**, *4*, 159−173.

(12) Garbajosa, J.; Tardajos, G.; Aircart, E.; Díaz Peña, M. *J. Chem. Thermodyn.* **1982**, *14*, 671−677.

(13) Silva, A. M. G.; Soares, V. A. M.; Calado, J. C. G. *J. Chem. Soc., Faraday Trans.* **1991**, *87*, 755−760.

(14) Press, W. H.; Flannery, B. P.; Teukolsky, S. A.; Vetterling, W. T. *Numerical Recipes: The Art of Scientific Computing*; Cambridge University Press: New York, 1988.

(15) Vetterling, W. T.; Teukolsky, S. A.; Press, W. H.; Flannery, B. P. *Numerical Recipes: Example Book [FORTRAN]*; Cambridge University Press: New York, 1989.

(16) Slack, G. A. *Z. Kristallogr.* **1983**, *165*, 1−22.

(17) McClellan, A. L.; Hansberger, H. F. *J. Colloid Interface Chem.* **1967**, *23*, 577−599.

(18) Everett, D. H. *Trans. Faraday Soc.* **1965**, *61*, 2478−2495.

(19) Sircar, S.; Myers, A. L. *J. Phys. Chem.* **1970**, *74*, 2828−2835.

(20) Rochester, C. H.; Yong, G. H. *J. Chem. Soc., Faraday Trans. 1* **1980**, *76*, 1158−1165.

(21) Sokoll, R.; Hobert, H.; Schmuck, I. *J. Catal.* **1990**, *125*, 276−284.

(22) Sokoll, R.; Hobert, H. *J. Catal.* **1990**, *125*, 285−291.

(23) Meyer, A. Y. *J. Chem. Soc., Perkin Trans. 2* **1985**, 1161−1169.

(24) Meyer, A. Y. *Chem. Soc. Rev.* **1986**, *5*, 449−474.

(25) Meyer, A. Y. *Struct. Chem.* **1990**, *1*, 265−279.

(26) Kharakoz, D. P. *J. Solution Chem.* **1992**, *21*, 569−595.

(27) Bondi, A. *J. Phys. Chem.* **1964**, *68*, 441−451.

(28) (a) *CRC Handbook of Chemistry and Physics*, 78th ed.; Lide, D. R., Ed.; CRC Press Inc.: Boca Raton, FL, 1997; pp 6−127. (b) *CRC Handbook of Chemistry and Physics*, 78th ed.; Lide, D. R., Ed.; CRC Press Inc.: Boca Raton, FL, 1997; pp 6−128.

(29) Dias-Peña, M.; Tardajos, G. *J. Chem. Thermodyn.* **1979**, *11*, 441−445.

(30) Caceres Alonso, P.; Caceres Alonso, M.; Nuñez Delgado, J. *J. Chem. Thermodyn.* **1986**, *18*, 629−633.

(31) Kumar, K. *Chem. Phys. Lett.* **1971**, *9*, 504−507.

(32) Amorim da Costa, A. M.; Batista de Carvalho, L. A. E.; Teixeira-Dias, J. J. C.; Barbosa, E. F. G.; Lampreia, I. M. S. *Can. J. Chem.* **1987**, *65*, 384−389.

(33) Lampreia, I. M. S.; Ferreira, L. A. V. *J. Chem. Soc., Faraday Trans.* **1996**, *92*, 47−51.

(34) Kumar, A.; Prakash, O.; Prakash, S. *J. Chem. Eng. Data* **1981**, *26*, 64−67.